Few-Body Syst (2019) 60:41
https://doi.org/10.1007/s00601-019-1509-9

Bernard L. G. Bakker · Chueng-Ryong Ji

The Compton Form Factors of the ^{4}Helium Nucleus

Received: 2 April 2019 / Accepted: 30 April 2019 / Published online: 20 May 2019

Abstract The number of Compton form factors of a scalar hadron is known to be three. It may be expected that depending on the structure of that hadron, it may occur that in some kinematical regimes the observables are only sensitive to one dominant form factor. Here we show in a particular kinematic situation that one may perform an experiment that unequivocally answers the question whether other form factors besides the anticipated dominant one can be neglected or not.

1 Introduction

Since the pioneering papers by Müller, by Radyuskin, and by Ji [1–3], a wealth of literature has appeared about generalized parton distributions (GPDs) in hadronic physics. These quantities are generally understood to provide more information about the quark content of hadrons beyond the parton distribution functions (PDFs) obtained in deep-inelastic scattering (DIS). A particular process to obtain GPDs is deeply-virtual Compton scattering (DVCS), which has been proposed to determine this information. One experimental set up is that a hard photon, $q^2 = -Q^2$, with Q much larger than the characteristic hadronic scales, hits the hadronic target with very small momentum transfer to the target, i.e., small Mandelstam $t \ll Q^2$. The detection of the outgoing real photon and hadron provides the information about the GPDs. It is important to realize that GPDs are not invariant quantities, as they are based on the idea that the so-called handbag diagram determines the amplitudes. The quantities that are invariant, like the electromagnetic form factors, are the Compton form factors (CFFs).

It is understood, however, that for large Q and for small Mandelstam t, each Compton form factor is related to a GPD. Thus the number of GPDs is equal to the number of CFFs. In the work by Tarrach and by Metz [4,5], a method is given for the determination of that number. It was found that in the case of electroproduction of a real photon, i. e., the reaction $h(e, e'\gamma)h$ on a spin =1/2 hadron the number of CFFs is twelve, while for a spineless target this number is three. In more recent literature [6–8] the latter number was corroborated. In a recent paper [9] we discussed the number of invariants occurring in the amplitudes for meson electro-production on a scalar target and emphasized that this number depends on the spin and parity of the produced meson.

In a recent preprint [10], it was proposed to study the partonic structure of ^{4}He in DVCS and determine its (only) chiral-even GPD, H_A. This experiment hinges on the assumption that besides the CFF that is related to

This article belongs to the Topical Collection “Ludwig Faddeev Memorial Issue”.

B. L. G. Bakker (✉)
Faculty of Science, Vrije Universiteit, Amsterdam, The Netherlands
E-mail: b.l.g.bakker@vu.nl

C.-R. Ji
Department of Physics, North Carolina State University, Raleigh, NC 27695-8202, USA
E-mail: crji@ncsu.edu

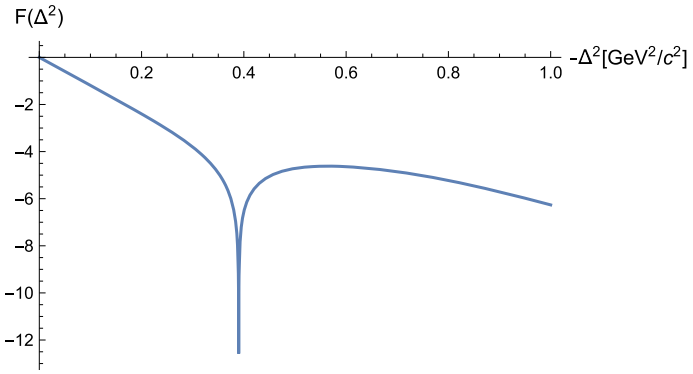

Fig. 1 The logarithm of the ^{4}He electromagnetic form factor according to Ref. [13]. $F(\Delta^2) = [1 - (a^2\Delta^2)^6]\exp(b^2\Delta^2)$, $a = 1.6014\,[\mathrm{GeV}/c]^{-1}$, $b = 3.45112\,[\mathrm{GeV}/c]^{-1}$

H_A, the other two CFFs are not significant in the proposed experiment. The analysis of the data on which this proposal is based is given in the paper by Liuti and Taneja [11]

A complication in DVCS is the fact that the DVCS amplitude is coherent with the Bethe–Heitler (BH) amplitude, which describes the process where the real photon in the final state is not emitted by the hadron (VCS), but by the (recoiling) electron. In the case of a target with a unique CFF, this complication can be used to determine the CFF by measuring the beam-spin asymmetry (BSA). This asymmetry occurs owing to the interference of the VCS and the BH amplitude. Recently [12] the BSA was measured.

In the BH amplitude, the electromagnetic structure of the target is probed only by the virtual photon emitted by the electron. Therefore, this amplitude contains the electromagnetic form factor (EMFF). As it is known that the ^{4}He form factor has nodes [13], the opportunity exists to check unequivocally the importance of CFFs beyond the leading one. In an experiment where the momentum squared of the photon hitting the hadron, $-\Delta^2$ corresponds to a node of the ^{4}He EMFF, the BH amplitude vanishes and thus the BSA vanishes too, if only one CFF contributes to the amplitudes. If in this kinematics a non-vanishing BSA still occurs, the existence of at least two CFFs is established. The only loop hole in the argument is the possibility that for some miraculous reason all CFFs have the same phase.

We studied the BSA in DVCS on ^{4}He for kinematics where the $-\Delta^2 = 0.390\mathrm{GeV}^2/c^2$, which is the point where the first node of the EMFF occurs (Fig. 1). To further fix the kinematics we specified the kinematics to values of the Bjorken variable $x_{\mathrm{Bj}} = 0.16, 0.23, 0.29$, and 0.39 as in Ref. [14].

Below we describe the necessary formalism, show the results and present our conclusions.

2 Tensor formalism

In virtual Compton scattering, the hadronic parts of the physical amplitudes are written as contractions of a tensor with the polarization vectors of the photons:

$$A^{\mathrm{had}}(h',h) = \epsilon^*(q';h')_\mu T^{\mu\nu}\epsilon(q;h)_\nu \quad \text{with} \quad q'_\mu T^{\mu\nu} = 0, \quad T^{\mu\nu}q_\nu = 0 \quad (i.e.,\ T^{\mu\nu}\ \text{transverse}), \tag{1}$$

where $q(q')$ is the momentum of the incoming(outgoing) photon. We shall also need the momenta of the incoming and recoiled hadron: p and p', respectively. It is also useful to introduce the momentum $\bar{P}$, defined as $\bar{P} = p + p'$.

The tensor is expressed in terms of CFFs and basis tensors. It is important to use the most general form of that tensor operator consistent with EM gauge invariance, as discussed by Tarrach and by Metz [4,5]. Recently, we introduced an alternative form of the Compton tensor [8], that circumvents some issues of the Tarrach and Metz construction. In this paper we use Tarrachs method. The tensor $T^{\mu\nu}$ is found by applying a two-sided projector $\tilde{g}^{\mu\nu}(q,q')$ to the most general second rank tensor expressed in terms of our basis:

$$T^{\mu\nu} = \tilde{g}^{\mu m}\, t_{mn}\, \tilde{g}^{n\nu}, \quad t_{mn} = t_0\, g_{mn} + \sum_{i,j} t_{ij}\, k_{i\,m} k_{j\,n} \quad \text{with} \quad \tilde{g}^{\mu\nu}(q,q') = g^{\mu\nu} - \frac{q^\mu q'^\nu}{q\cdot q'}. \tag{2}$$

We define the reduced momenta, ($k \in \{\bar{P},\ q',\ q\}$):

$$\tilde{k}^{\mu}_{\rm L} = \tilde{g}^{\mu m} k_m, \quad \tilde{k}^{\nu}_{\rm R} = k_n\, \tilde{g}^{n\nu} \tag{3}$$

and find for the case where the outgoing photon is real, $q'^2 = 0$, the following result for $T^{\mu\nu}$

$$T^{\mu\nu} = \mathcal{H}_0\ \tilde{g}^{\mu\nu} + \mathcal{H}_1\ \tilde{P}^{\mu}_{\rm L}\, \tilde{P}^{\nu}_{\rm R} + \mathcal{H}_2\ \tilde{P}^{\mu}_{\rm L} \tilde{q}^{\nu}_{\rm R}. \tag{4}$$

Contracting the tensor with $\epsilon^*_\mu(q')$ and $\epsilon_\nu(q)$ we find that all three pieces of the tensor contribute to the amplitudes. The number of independent tensor structures is equal to the number of independent physical matrix elements, namely $A(1,1),\ A(1,0),\ A(1,-1)$, which is consistent with parity conservation: $A(-h',-h) = (-1)^{h'-h} A(h',h)$, $h' = \pm 1, h = \pm 1, 0$.

The tree-level DVCS amplitudes corresponding to Tarrach's formulation to the CFFs are given by

$$\mathcal{H}_0^{\rm tree} = -2,\ \mathcal{H}_1^{\rm tree} = \frac{1}{s_{\rm had} - M^2} + \frac{1}{u_{\rm had} - M^2},\ \mathcal{H}_2^{\rm tree} = 0, \tag{5}$$

where $s_{\rm had} = (p+q)^2,\ u_{\rm had} = (p-q')^2$, and M is the target hadron's mass.

The complete VCS amplitudes are given as convolutions of the hadronic part and the leptonic part, the latter describing the emission of a virtual photon by an electron with momentum k, the recoiling electron having momentum k' given by $k' = k - q$.

We shall not discuss the amplitudes here. The hadronic parts were given explicitly in Ref. [15].

3 Kinematics

To understand what is at stake when the experiments are analyzed in terms of GPDs, one must keep in mind that such an analysis can succeed only when the virtuality $-Q^2$ of the incoming photon is much larger than any other physical scale, allowing to take the $Q \to \infty$ limit. Moreover, it is understood that the Mandelstam variable $t_{\rm had}$ is small compared to Q^2. Such kinematics is sometimes denoted as the DVCS limit.

This point has been discussed in our earlier review [16]. The relevant points are as follows: all three hadronic Mandelstam variables, $s_{\rm had}$, $t_{\rm had}$, and $u_{\rm had}$ scale as Q^2 for asymptotic Q. There are two consequences. First, $\mathcal{H}_1^{\rm tree}$ scales as $1/Q^2$ compared to $\mathcal{H}_0^{\rm tree}$. This difference in scaling behaviour could be taken as meaning that in the VCs limit one may neglect the contribution of $\mathcal{H}_1^{\rm tree}$. However, that is not a valid conclusion, because the corresponding basis tensors $T_0^{\mu\nu} = \tilde{g}^{\mu\nu}$ and $T_1^{\mu\nu} = \tilde{P}^{\mu}_{\rm L}\, \tilde{P}^{\nu}_{\rm R}$ have the opposite scaling properties. (This is obvious if one keeps in mind that the parts of the amplitudes corresponding to these two CFFs must have the same dimensions.) Thus, at the phenomenological level, there is no reason to expect that these two contributions to the amplitudes have very different scaling behaviours. A second point concerns the scaling of $t_{\rm had}$. In terms of the invariants and the cosine of the photon scattering angle $\theta_{\rm C}$ in the center-of-mass frame with the z-axis along the three-momentum of the incoming virtual photon it is given by

$$t = -\frac{Q^2\left[Q^2(1-x_{\rm Bj}) + 2M^2 x_{\rm Bj}^2 - Q(1-x_{\rm Bj})\sqrt{Q^2 + 4M^2 x_{\rm Bj}^2}\cos\theta_{\rm C}\right]}{2x_{\rm Bj}\left[Q^2(1-x_{\rm Bj}) + M^2 x_{\rm Bj}\right]}, \tag{6}$$

where M is the mass of the hadronic target. If Q becomes large, this expression reduces to

$$t_{\rm had} \to -\frac{1-\cos\theta_{\rm C}}{2x_{\rm Bj}}\, Q^2 + \mathcal{O}(M^2). \tag{7}$$

This result shows that $t_{\rm had}$ can only be negligible if the scattering angle is taken to be of order $1/Q$ and, moreover, the mass M is much smaller than Q. This requirement puts a severe limit on the set up of the experiments purporting to determine the GPDs.

On the other hand, CFFs are Lorentz-invariant quantities that do not depend on a special kinematics. In any kinematics the experimental data can be analyzed in terms of CFFs, which in general depend on the Mandelstam variables.

The kinematics we have used in the numerical calculations is inspired by the kinematics in Ref. [14]. In that experiment the data were taken for the following kinematical values: $x_{\rm Bj} \in \{0.16, 0.23, 0.29, 0.39\}$,

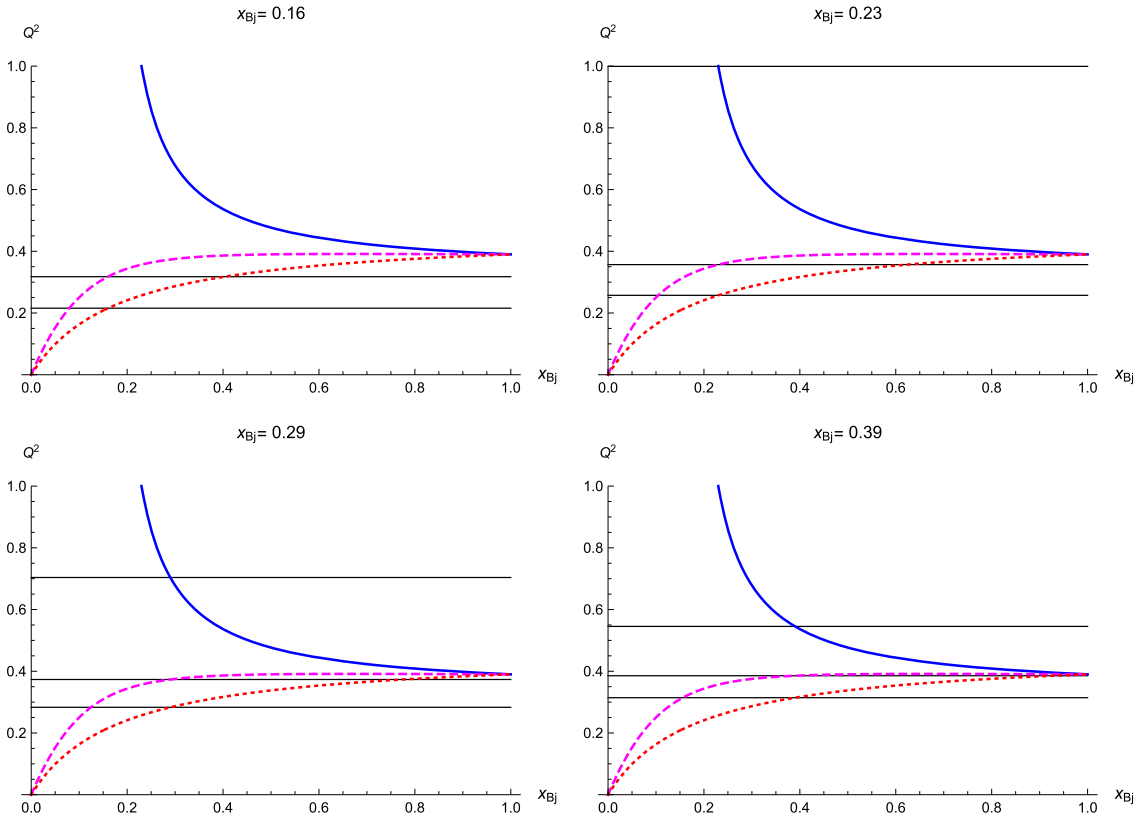

Fig. 2 Kinematical domains for four values of x_{Bj}. The solid curve is for $\theta_C = 0$, the dashed one for $\theta_C = \pi/2$ and the dotted curve for $\theta_C = \pi$. The thin black lines represent the values of Q^2 in GeV^2/c^2 for which $\Delta^2 = -0.390$ GeV$^2/c^2$

$-t_{had} \in \{0.14, 0.28, 0.49, 1.08\}$, and $Q^2 \in \{1.40, 1.89, 2.34, 3.09\}$. Because we aimed to show that it is possible to do a *crucial experiment showing that the BSA also occurs when there is no interference with the BH process*, we kept the value of $t_{had} = \Delta^2$ fixed at the node of the ^{4}He form factor, i.e., $t_{had} = -0.390\,\text{GeV}^2/c^2$. Then for a given beam energy–we take 11 GeV–and using the ^{4}He mass 3.7284 GeV/c^2 we can find the locus in the (x_{Bj}, Q^2)-plane where t_{had} has this value. In this domain, the points can be labeled by θ_C. In the spirit of the usual DVCS limit, we limited our calculations mainly to small values of θ_C: 5° and 10°, and for demonstrating the effect of taking a larger angle we also show the results for $\theta_C = 90°$.

4 Numerical calculations

4.1 Kinematical domains

First, we show the kinematical domains for fixed beam energy, target mass and the four values of x_{Bj} namely 0.16, 0.23, 0.29, and 0.39. In the case of $x_{Bj} = 0.16$ the value of Q^2 for which $t_{had} = -0.390$ GeV^2/c^2 for $\theta_C = 0$ is equal to 8.88167 GeV^2/c^2 and therefore not shown in Fig. 2.

The minimum value of t_{had} is obtained for θ_C equal to 0. In view of the geometrical limitations of the detector systems, we performed our calculations of the BSA to *small angles but not exactly 0*. In particular, we did calculations for $\theta_C = \pi/36$ and $\theta_C = \pi/18$. We show our results in the next section (Fig. 3).

4.2 Beam-spin asymmetries

As up till now little is known about the CFFs of ^{4}He, we took as our model the tree-level expressions given in Eq. (5). As expected, the BSA vanishes in this approximation, because both non vanishing CFFs are real.

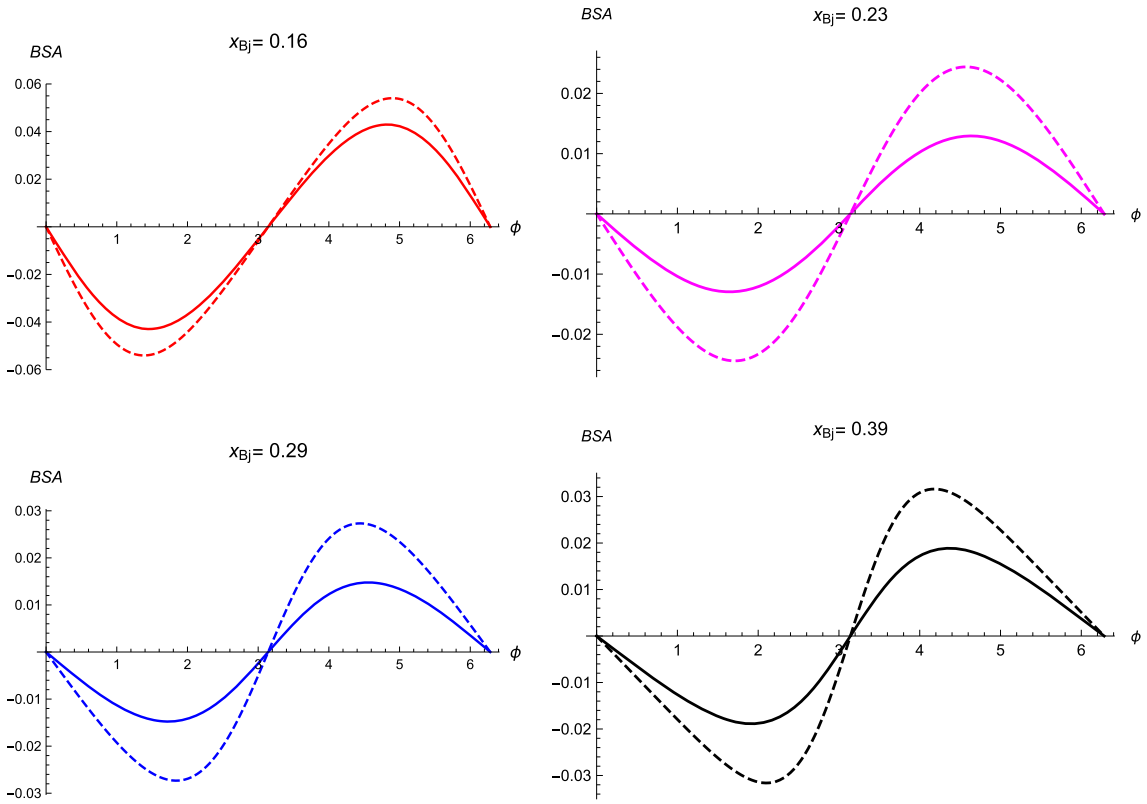

Fig. 3 Beam-spin asymmetry (BSA) for four values of $x_{\rm Bj}$, the solid line is for $\theta_{\rm C} = \pi/36$, the dashed line for $\theta_{\rm C} = \pi/18$

It is to be expected that owing to the hadronic structure of the target, the CFFs will develop imaginary parts. Thus, to produce a benchmark result we multiplied the CFF $\mathcal{H}_0^{\rm tree}$ with the factor $1 + i$ in all cases for which we calculated the BSA. It is obvious that alternatively we could have multiplied $\mathcal{H}_1^{\rm tree}$ with the same factor, but keep $\mathcal{H}_0^{\rm tree}$ real and obtain the same BSA, because this observable is proportional to the product of the two CFFs.

In Fig. 3 we show the results for the four different values of the Bjorken variable. First we note that the BSAs, although being small, do not vanish. Secondly, although the BSA shows the node of $\sin\phi$, the full shape demonstrates that on increasing $x_{\rm Bj}$, higher Fourier components become more important. Thirdly, we see that the BSA increases at all angles when the scattering angle increases.

To see how this change in the shape of the BSA is modified when non-forward kinematics is adopted, we show in Fig. 4 the previous results for $\theta_{\rm C} = \pi/36$ together with the BSA at $\theta_{\rm C} = \pi/2$.

It is clear that somewhere in the forward hemisphere $\mathcal{H}_1^{\rm tree}$ changes sign. When one calculates the full kinematics, one finds that the node in this CFF occurs for an angle $\theta_{\rm C}$ given by

$$\cos\theta_{\rm C} = \frac{(1 - 2x_{\rm Bj})\,Q}{\sqrt{Q^2 + 4M^2 x_{\rm Bj}^2}}. \tag{8}$$

For the kinematics we have used here this angle lies between $0.301461\,\pi$ at $x_{\rm Bj} = 0.16$ and $0.485374\,\pi$ at $x_{\rm Bj} = 0.39$.

5 Summary and conclusions

We have calculated the beam-spin asymmetries in virtual Compton scattering on a scalar target. The target was modelled by using the Compton form factors for a structureless scalar particle with mass M and charge equal to twice the proton charge. The number of CFFs is two in the structureless case. If we introduce an imaginary

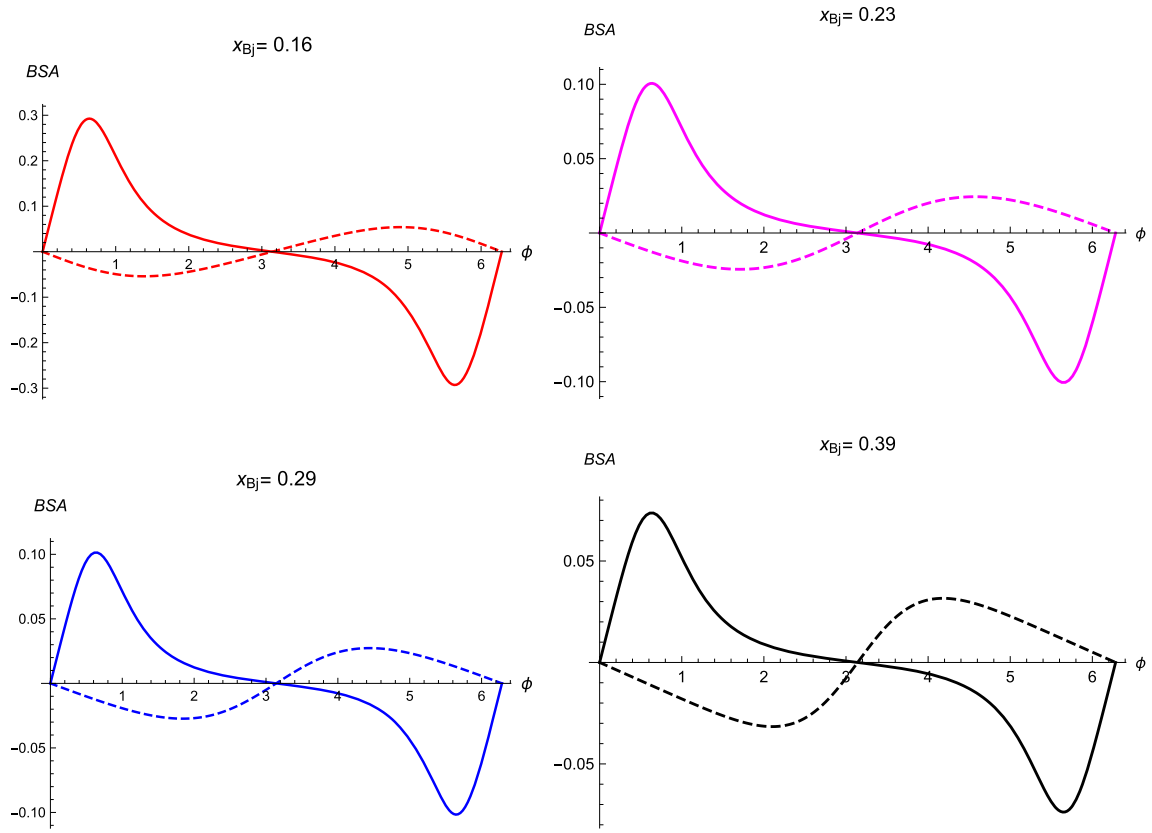

Fig. 4 Beam-spin asymmetry for the four values of x_{Bj}, the dashed line is for $\theta_C = \pi/36$, the solid line for $\theta_C = \pi/2$

part to one of the these CFFs, there exists a small but finite BSA. In general this BSA may be obscured by the interference of the virtual Compton amplitude with the coherent Bethe–Heitler amplitude. In a special kinematics, enabled by the fact that the charge form factor of the ^{4}He nucleus has a node, and consequently the Bethe–Heitler amplitude vanishes, one can measure the BSA produced by the virtual Compton scattering alone.

By performing our calculation in the kinematical regime covered by recent experiments at the Jefferson Lab, we have shown that the kinematics for this crucial experiment can be realized, showing unequivocally that at least two Compton form factors contribute to virtual Compton scattering. This conclusion implies that in the analysis of the experimental data a limitation to a purportedly dominant Compton form factor introduces a systematic error in the determination of this CFF.

References

1. D. Müller, D. Robaschik, B. Geyer, F.M. Dittes, J. Horesji, Wave functions, evolution equations and evolution kernels from light ray operators of QCD. Fortschr. Phys. **42**, 101 (1994)
2. A.V. Radyushkin, Scaling limit of deeply virtual Compton scattering. Phys. Lett. **380**, 417 (1996)
3. X.-D. Ji, Gauge-invariant decomposition of nucleon spin. Phys. Rev. Lett. **78**, 610 (1997)
4. R. Tarrach, Invariant amplitudes for virtual Compton scattering off polarized nucleons free from kinematic singularities, zeros and constraints. Nuovo Cimento **28 A**, 409 (1975)

5. A. Metz, Virtuelle Comptonstreuung und die Polarisierbarkeiten des Nukleons (in German). Ph. D. Thesis, Universität Mainz, (1997)
6. A.V. Belitsky, D. Müller, Refined analysis of photon leptoproduction off a spinless target. Phys. Rev. D **79**, 014017 (2009)
7. K. Kumerički, D. Müller, Deeply virtual Compton scattering at small x_B and the access to the GPD H. Nucl. Phys. B **841**, 1 (2010)
8. B.L.G. Bakker, C.-R. Ji, The construction of Compton tensors in scalar QED. Few-Body Syst. **58**, 1 (2017)
9. C.-R. Ji, H.-M. Choi, A. Lundeen, B.L.G. Bakker, Beam spin asymmetry in electroproduction of pseudoscalar or scalar meson production off the scalar target. Phys. Rev. D (to be published)
10. W.R. Armstrong et al., CLAS Collaboration, Partonic Structure of Light Nuclei, arXiv:1708.00888v2 [nucl-ex] (2017)
11. S. Liuti, S.K. Taneja, Micoscopic description of deeply virtual Compton scattering off spin-0 nuclei. Phys. Rev. C **72**, 032201(R) (2005)
12. M. Hattawy, et al., CLAS Collaboration, First Exclusive Measurement of Deeply Virtual Compton Scattering off ^{4}He: Toward the 3D Tomography of Nuclei, Phys. Rev. Lett, **119**, 202004 (2017)
13. R.F. Frosch, J.S. McCarthy, R.E. Rand, M.R. Yearian, Structure of the He^4 nucleus from elastic electron scattering. Phys. Rev. **60**, 874 (1967)
14. M. Hattawy, et al., CLAS Collaboration, Deeply Virtual Compton Scattering measurement off bound protons, arXiv:1812.07628v1 [nucl-ex] (2018)
15. B.L.G. Bakker, C.-R. Ji Extraction of Compton form factors in scalar QED. Few-Body Syst. **56**, 275 (2015)
16. C.-R. Ji B.L.G. Bakker, Conceptual issues concerning generalized parton distributions. Int. J. Mod. Phys. E **22**, 1330002 (2013)